The Effect of Salts on the Stability of the H2A−H2B Histone Dimer

Lisa M. Gloss* and Brandon J. Placek

School of Molecular Biosciences, Washington State University, Pullman, Washington 99164-4660

Received June 11, 2002; Revised Manuscript Received September 27, 2002

ABSTRACT: The core nucleosome, which comprises an H3−H4 tetramer and two H2A−H2B dimers, is not a static DNA packaging structure. The nucleosome is a dynamic protein−DNA complex, and the modulation of its structure is an important component of transcriptional regulation. To begin to understand the molecular details of nucleosome dynamics, we have investigated the stability of the isolated H2A−H2B dimer. The urea-induced equilibrium responses of the heterodimer have been examined by far-UV circular dichroism and intrinsic tyrosine fluorescence. The two spectroscopic probes yielded coincident transitions, and global fitting of the reversible urea-induced unfolding further demonstrated that H2A−H2B unfolds by a two-state equilibrium response. At physiological ionic strengths, the free energy of unfolding in the absence of urea of H2A−H2B is 11.8 ± 0.3 kcal mol^{-1}, moderate stability for a dimer of 26.4 kDa. The *m* value, or sensitivity of the unfolding to urea, is 2.9 ± 0.1 kcal mol^{-1} M^{-1}. This value is significantly larger than would be predicted for the unfolding of the dimerization motif alone (∼2 kcal mol^{-1} M^{-1}), suggesting that the N-terminal tails may adopt a collapsed, solvent-excluding structure that undergoes an unfolding transition. The efficacies of several potassium salts and three chloride salts to stabilize the H2A−H2B dimer were determined. The salt-dependent stabilization of the H2A−H2B dimer shows that the Hofmeister effect is the predominant mode of stabilization. However, studies employing multiple salts suggest that there is a component of stabilization that must arise from screening of electrostatic repulsion in the highly basic heterodimer. The most highly charged regions of the dimer are the N-terminal tails, sites of posttranslational modifications such as acetylation and phosphorylation. These modifications, which alter the charge density of the tails, are involved in regulation of nucleosome dynamics.

Many essential functions in the cell are performed by oligomeric proteins and macromolecular protein assemblies. These multimeric structures have evolved, in part, because of their regulatory and functional advantages over individual subunits. Examples of these advantages include allosteric mechanisms, cooperative binding of ligands, channeling of substrates in metabolic pathways, or the very precise control of the DNA chemistries in the cell, such as DNA repair, replication, and transcription. Understanding the function and regulation of these complexes requires biophysical characterization of the assembly and stability of the component proteins of the complexes.

Many insights into the stability of proteins have been gained from studies on small monomeric systems. However, dimeric and higher-order oligomeric systems are an important extension of the studies of protein stability; the stability of oligomeric proteins exhibit a protein-concentration dependence and a coupling between quaternary interactions across an intermolecular interface and secondary and tertiary structural interactions. What is the interplay between the stability of the oligomerization interface and stability within the isolated monomeric chain? Is the folding of the oligomer a two-state equilibrium between folded oligomer and unfolded monomers? Or can partially folded monomers be populated under conditions that disrupt the oligomeric interface?

An important mediator of the accessibility of DNA in an eukaryotic cell is the nucleosome, the basic packaging unit of chromatin. The eukaryotic core nucleosome contains an H3−H4 heterotetramer, two H2A−H2B heterodimers, and ∼160 basepairs of DNA. The stability, structure, and association state of the proteins of the core nucleosome play an important role in transcriptional regulation (*1*, *2*). The core histones represent a system well suited for investigating the folding mechanism of oligomeric proteins and macromolecular assembly.

All four core histones contain the same dimerization motif: a long central α-helix, flanked on the N and C terminii by a loop, and a shorter α-helix (Figure 1). Two monomers dimerize in an intertwined, head-to-tail manner that has been termed a "handshake motif" (*3*). Many of the contacts in the hydrophobic core of the dimer are intermolecular, between the two polypeptides. Sequence analyses and three-dimensional structure determinations have demonstrated that this dimerization motif is found in many proteins involved in macromolecular protein-DNA assemblies (*4*−*7*). The core histones also contain flexible N-terminal tails that are not completely resolved in the X-ray crystal structure of the core nucleosome (*8*). The tails of all four core histones are the sites of the various posttranslational modifications that modulate the repressive nature of chromatin (*9*, *10*). In

† This work was supported by grants to L.M.G. from the American Cancer Society (RPG-00-085-01-GMC) and the National Science Foundation (MCB-9983831). B.J.P. was partially supported by an NIH Biotechnology training grant (GM08336-13).

* Corresponding author. Phone (509) 335-5859. FAX (509) 335-9688. E-mail: lmgloss@wsu.edu.

10.1021/bi026282s CCC: $22.00
Published on Web 11/19/2002

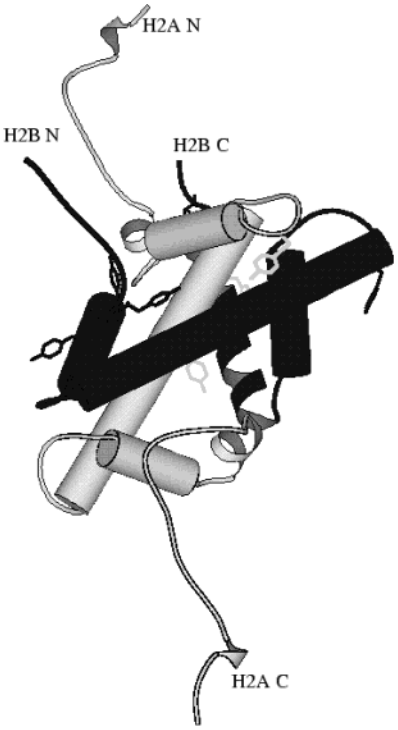

FIGURE 1: Ribbon diagram of the H2A−H2B dimer, derived from the X-ray crystal structure of the core nucleosome (*8*). The H2A monomer is shown as the lighter colored chain. The α-helices of the histone fold motif are represented as cylinders. The H2A chain depicts residues 4−118 (of 129 residues), and that of H2B, residues 24−122 (of 122 residues). The three and five Tyr residues of the H2A and H2B monomers, respectively, are displayed in stick representations. The figure was rendered using Molscript v2.1 (*57*).

addition to their N-terminal tails, H2A and H2B have C-terminal sequences that extend beyond the histone fold. The H2A C-terminal 31 residues adopt a largely extended conformation; the H2B C-terminal extension of 23 residues is predominantly helical (Figure 1).

The structural and thermodynamic characterization of the interactions between the intact histone oligomers, in the presence and absence of DNA, has been the subject of many studies (for review and examples, see refs *11*−*16*). The stability of the isolated H2A−H2B dimer and H3−H4 dimer (populated at lower pH) has been examined by thermal denaturation using CD[1] and differential scanning calorimetry (*17*−*19*). These previous studies showed that both heterodimers were stabilized by increases in ionic strength, using NaCl for both systems and sodium acetate for the H3−H4 dimer at pH 4.5. However, these studies did not establish the mechanism by which salts stabilize the histone dimers.

Salts can affect protein stability by two common mechanisms: (1) by altering the interactions of the aqueous solvent with the protein through preferential hydration (in the model of Timasheff and colleagues (*20*, *21*)), also called the Hofmeister effect (for review, see refs *22* and *23*); and (2) by screening electrostatic interactions between charged amino acids on the protein surface. Stabilization by altering the activity of water, and thus enhancing the hydrophobic effect, should be common to most proteins. Electrostatic screening can be destabilizing in the presence of favorable electrostatic interactions or salt-bridges (for example, ref *24*). Salts can also stabilize a protein by screening destabilizing electrostatic repulsion between like-charged residues, such as seen for *Bacillus subtilus* cold shock protein B (*25*). The potential of an electrostatic mechanism of salt stabilization is of particular interest in the case of the histone oligomers. These proteins are highly basic, as expected for proteins that form macromolecular complexes with a poly-anion such as DNA, with the highest charge density being in the N-terminal tail regions.

In this study, we examine the stability of the isolated H2A−H2B heterodimer using urea denaturation in the presence of a variety of salts. The results presented here show that the salt stabilization of the H2A−H2B dimer involves a combination of enhancing the hydrophobic effect (via the Hofmeister effect or preferential hydration) and screening of electrostatic repulsion.

MATERIALS AND METHODS

Materials. Ultrapure urea was purchased from ICN Biomedicals (Costa Mesa, CA). CM-Sepharose resin was purchased from Sigma (St. Louis, MO); Sephacryl S-100 and Heparin resins were purchased from Amersham Pharmacia (Uppsala, Sweden). All other chemicals were of reagent-grade.

Methods. Recombinant H2A and H2B proteins were overexpressed in the *E. coli* strain, BL21(DE3) pLysS, using the T_7pET vectors with the *Xenopus laevis* genes, constructed by Luger et al. (*26*); the proteins were expressed individually and extracted from inclusion bodies as described previously (*26*). The subsequent purification of the histone proteins was accomplished by a procedure modified from that published previously. All chromatography steps were performed at room temperature. The inclusion body fraction, after solubilization in 6 M guanidine HCl, was applied to a S-100 column equilibrated in Buffer A (6 M urea, 20 mM potassium phosphate, 50 mM NaCl, 1 mM EDTA, pH 7.2). After elution from the S-100 column, the fractions containing histone protein were pooled and applied to a CM-Sepharose column equilibrated in Buffer A. Histone proteins were eluted with a gradient of NaCl from 50 to 600 mM NaCl. The histone-containing fractions were ∼90% pure, as judged by SDS polyacrylamide electrophoresis, after this second column. For storage, the histones were dialyzed into 10 mM HCl and lyophilized if concentrating the protein was necessary. To reconstitute the H2A−H2B dimer, stocks of H2A and H2B monomers in 10 mM HCl were mixed at equimolar concentrations and then rapidly diluted with buffer containing 20 mM potassium phosphate, 50 mM KCl, 1 mM EDTA, pH 7.2. The refolded dimer was then applied to a Heparin column equilibrated with the above refolding buffer; the column was washed with buffer containing 1 M KCl, and the folded histones were eluted with a buffer containing 2 M KCl. (Similar results were obtained with NaCl containing buffers.) Heparin chromatography further purified the histones and removed any misfolded protein, which remained

[1] Abbreviations: CD, circular dichroism; C_M, the urea concentration at which the apparent fraction of unfolded monomer constitutes 50% of the population; ΔASA, change in solvent-accessible area between the native and unfolded species of proteins; $\Delta G°$ (H_2O), the free energy of unfolding in the absence of denaturant; F_{app}, apparent fraction of unfolded monomer; FL, fluorescence; KOAc, potassium acetate; KPi, potassium phosphate, pH 7.2; *m* value, parameter describing the sensitivity of the unfolding transition to the [Urea]; MRE, mean residue ellipticity; std. dev., standard deviation.

bound to the column until washed with 6 M guanidine HCl. The misfolded species were generally aggregated homooligomers. The Isenberg lab demonstrated that H2A and H2B can form homodimers; however, these species have a much weaker association than the heterotypic dimer and are prone to aggregation (*11*). The Heparin purification removed these aggregated homodimers and other minor impurities, yielding histone heterodimers that were >95% pure, as judged by SDS polyacrylamide electrophoresis. The homogeneity of the reconstitution to the dimeric state of the H2A and H2B monomers was confirmed by HPLC size-exclusion chromatography.

The conditions for all of the equilibrium unfolding experiments were a buffer of 20 mM potassium phosphate, pH 7.2, with 0.1 mM EDTA and a temperature of 25 °C. Fluorescence data were collected on an AVIV Model ATF-105/305 differential/ratio spectrofluorometer; circular dichroism data were collected on an AVIV 202SF spectrophotometer. Fluorescence data were collected with an excitation wavelength of 280 nm and emission was monitored at 305 to 306 nm. CD data were collected at 220−225 nm. Equilibrium urea unfolding transitions were collected with an automated titrator interfaced with the Aviv spectrometers. The equilibration time at each urea concentration in the titrations was generally 2 or 3 min. These equilibration times are 50 times longer than the slowest kinetic folding phases observed for the H2A−H2B dimer (relaxation times of <2 s at urea concentrations equal to the C_M of the equilibrium transitions). The unfolding and refolding responses of the H2A−H2B dimer were complete within the deadtime of manual mixing methods, 2−5 s. The sufficiency of the equilibration times employed in the titrations was verified by performing the automated titrations with long and short equilibration times (~2-fold difference in the equilibration delay); the transitions monitored with the varied equilibration times were superimposable.

Equilibrium urea unfolding transitions were fitted to a two-state model for a dimeric system, using equations described elsewhere (for example, ref *27*). A linear extrapolation between the free energy of unfolding, $\Delta G°$, and the urea concentration was used (*28*):

$$\Delta G° = \Delta G°(H_2O) - m[\text{Urea}] \quad (1)$$

where $\Delta G°(H_2O)$ is the free energy of unfolding in the absence of denaturant at a standard state of 1 M dimer and the *m* value reflects the sensitivity of the transition to the urea concentration. The data were fitted globally using the program Savuka 5.1, which has been described elsewhere (*29*, *30*). Rigorous analyses of the error surfaces of the global fits were performed as described elsewhere (*31*). The errors determined from this analysis were not perfectly symmetrical; however, there was only a small difference between the lower and upper limits. The reported errors represent one standard deviation of the average of the limits.

RESULTS

Spectral Properties of the H2A−H2B Dimer. The H2A−H2B dimer exhibits a far-UV CD spectra typical of an α-helical protein, with double minima at 208 and 222 nm, as published elsewhere (for example, following paper, Placek and Gloss, and ref *17*). Upon the addition of denaturants, the dimer unfolds and exhibits the relatively featureless CD spectra commonly observed for unfolded proteins (data not shown). Therefore, the far-UV CD signal between 220 and 225 nm is a useful probe for the secondary structure content of this heterodimer as a function of denaturant (Figure 2). The *Xenopus laevis* H2A and H2B histones contain 3 and 5 tyrosine residues, respectively, with no tryptophan residues. The Tyr residues are distributed throughout the primary structure of the histones, predominantly within the histone fold motif, and are involved in intra- and intermonomer contacts (Figure 1). There are no Tyr residues in the N-terminal tails of the histones. The emission maximum of the intrinsic Tyr fluorescence of the folded dimer is 305−306 nm. Fluorescence intensity decreases with increasing urea concentration, with negligible change in the wavelength of the emission maximum. FL intensity at 305 provides a sensitive measure of the tertiary and quaternary structure of the heterodimer in denaturation experiments (Figure 2).

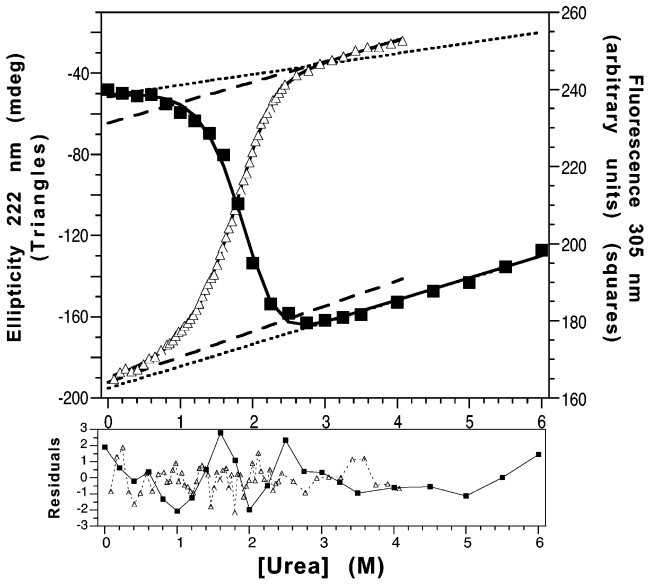

FIGURE 2: Urea-induced unfolding transitions of H2A−H2B monitored by FL and CD spectroscopy. FL 305 nm, ■; CD 222 nm, Δ. Folded and unfolded baselines are shown as dotted and dashed lines for the FL and CD data, respectively. The solid lines are the results of a global fit of 7 H2A−H2B equilibrium data sets (see Figure 3). Residuals are shown in the lower panel; similar or better residuals result from the fits of the data in other figures in this paper. Protein concentration is 5 μM dimer, i.e., 5 μM H2A monomer and 5 μM H2B monomer. Conditions: 20 mM potassium phosphate, 200 mM KCl, 0.1 mM EDTA, pH 7.2, 25 °C.

Stability of H2A−H2B in Buffer with 200 mM KCl. The equilibrium urea-induced unfolding responses of the H2A−H2B heterodimer were monitored by far-UV CD and intrinsic Tyr fluorescence. The equilibrium unfolding was highly reversible, with no evidence for hysteresis. This reversibility was demonstrated in two ways. (1) Urea-unfolded protein was diluted into low concentrations of urea (<1 M); 95−100% of CD and FL signals of native heterodimer were regained. (2) Automated titrations were performed in both the unfolding and refolding direction. Folded protein in the cuvette was titrated with a stock of unfolded protein, and conversely, unfolded protein in the cuvette was titrated with a stock of folded protein. The unfolding and refolding titrations were superimposable, as shown by the CD transitions in Figure 3A.

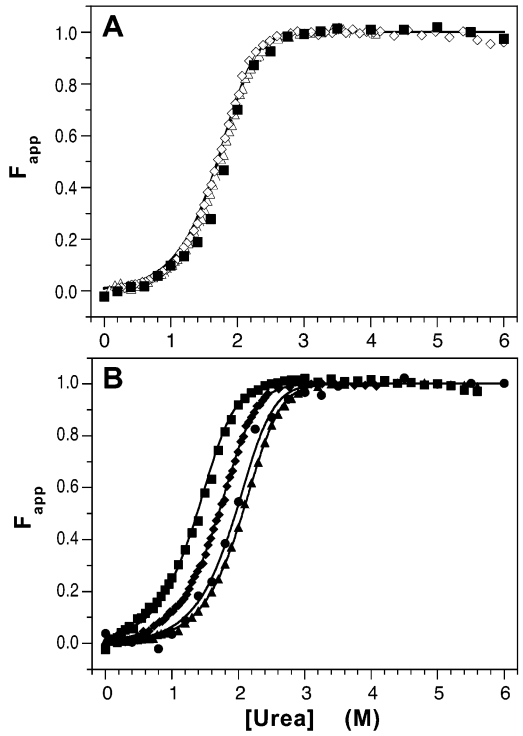

FIGURE 3: Representative H2A−H2B dimer urea equilibrium denaturation transitions. (A) Apparent fraction of unfolded monomers (F_{app}) as a function of urea concentration at 5 μM dimer. FL 305 nm, ■; CD 222 nm unfolding transition, Δ; CD 222 nm refolding transition, ◇. (B) Unfolding transitions at representative dimer concentrations. 1 μM FL data, ■; 5 μM CD data, ◆; 17.9 μM FL data, ●; 30 μM FL data, ▲. In both panels, the solid lines represent the global fit of seven H2A−H2B equilibrium data sets. The size of the data symbols, in this figure and Figure 4, are similar to the error of the data. Conditions are given in the legend of Figure 2.

The F_{app} curves of transitions monitored by both CD and FL probes were coincident (Figure 3A). This coincidence suggests that the heterodimer unfolds at equilibrium by a two-state response, i.e., the only populated states are native dimer and unfolded monomers. A data set of seven equilibrium transitions was collected over a range of concentrations from 1 to 30 μM dimer. The data were well described by global fitting to a two-state dimeric unfolding model, further confirming the lack of equilibrium intermediates in the urea-induced unfolding of H2A−H2B. Representative data with the results of the global fits (solid lines) are shown in Figure 3B. The global fitting yielded $\Delta G°(H_2O)$ and m values (eq 1, Methods) of 11.8 ± 0.3 kcal mol^{-1} and 2.9 ± 0.1 kcal mol^{-1} M^{-1}, respectively. These values are in good agreement with the average of the values determined from individual, local fits of the data, 11.9 kcal mol^{-1} (std. dev. 0.4) and 3.1 kcal mol^{-1} M^{-1} (std. dev. 0.1), respectively.

Effect of Salts on the Stability of the H2A−H2B Dimer. To obtain insights into the mechanism by which salts stabilize the H2A−H2B dimer, urea-induced equilibrium unfolding responses were determined as a function of salt concentration. A series of potassium salts with different anions were employed, as well as chloride salts with different cations (Table 1; Figures 4−6). Dimer concentrations of 10 or 5 μM were used; the protein concentration was the same for all data sets with a given salt. The equilibrium titrations were monitored primarily by intrinsic Tyr FL. At a subset of conditions, titrations were also monitored by far-UV CD.

Table 1: Equilibrium Urea Unfolding Parameters Determined with Various Salts[a]

salt	number of data sets	$\Delta(\Delta G°)/\Delta C_\mu$[b] (kcal mol^{-1} M^{-1})
KI	7	1.0 (0.1)
KBr	8	4.1 (0.3)
KCl	13	5.9 (0.3)
KOAc	8	6.6 (0.3)
KPi	11	9.7 (0.3)
K_2SO_4	6	10.2 (1.4)
NaCl	5	6.1 (0.7)
NH_4Cl	5	5.2 (0.2)

[a] Conditions: 20 mM potassium phosphate as buffer, 0.1 mM EDTA, pH 7.2, 25 °C, and 5 or 10 μM dimer. The values of $\Delta G°$ (H_2O) and $\Delta(\Delta G°)/\Delta C_\mu$ are not protein concentration dependent. Dimer concentrations were kept constant for all titrations collected with a given salt. [b] Slope of a linear fit of the parameter vs ionic strength. Data for $\Delta G°$ (H_2O) are shown in Figures 5 and 6. The values in parentheses represent the standard deviation for the linear fits of the data weighted by the error from rigorous error analysis of global fits (*31*) that determined the $\Delta G°$ (H_2O) and m values.

The CD transitions were superimposable with those monitored by FL (data not shown), demonstrating that salts do not alter the two-state unfolding equilibrium mechanism of H2A−H2B observed at 200 mM KCl. Unfolding and refolding titrations were collected at high salt concentrations and were superimposable, demonstrating no loss of reversibility in folding with increasing salt concentrations. Representative titrations in potassium chloride are shown in Figure 4A and potassium iodide and potassium phosphate in Figure 4B.

Initially, the data sets were fit locally, allowing both the $\Delta G°(H_2O)$ and m values to vary with the salt concentration. These analyses demonstrated that for all salts, the m value did not significantly change over the range of salt concentrations examined. However, there was a strong autocorrelation between the values fit for the $\Delta G°(H_2O)$ and m parameters. To minimize the effect of this auto-correlation on the salt-dependence of $\Delta G°(H_2O)$, the data sets were refit globally with the m value linked across all titrations collected for a given salt. Thus, the m value was treated as a salt-independent parameter. The average of the m values for the eight salts employed is 2.8 kcal mol^{-1} M^{-1} (std. dev. 0.2). The results of the global fits are represented by the lines in Figure 4. The C_M values were unaltered by local versus global fitting, further support for the validity of the global fitting of the data with a salt-independent m value.

For all salts, the value of $\Delta G°(H_2O)$ (Figures 5 and 6) and the C_M values (data not shown) increased linearly with ionic strength (and salt concentration). The slopes of the linear increases of $\Delta G°$ (H_2O) are a measure of the relative efficacy of the salts in stabilizing H2A−H2B and are given in Table 1. For the potassium salts, the ranking of the slopes, $\Delta(\Delta G°)/\Delta C_\mu$, follows the Hofmeister series: $SO_4^{2-} > PO_4^{2-} > OAc^- > Cl^- > Br^- > I^-$. The difference in the stabilization efficacy for KI versus K_2SO_4 is ~10 kcal mol^{-1} M^{-1} (Table 1). The H2A−H2B dimer stability is not very sensitive to the nature of the cation. The three chloride salts examined, NH_4Cl, KCl, and NaCl, differ in efficacy by less than 1 kcal mol^{-1} M^{-1} (Figure 5B, Table 1). This insensitivity demonstrates that anions are more important than cations to the stability of the dimer. The Hofmeister series ranks the cations employed, from most stabilizing to

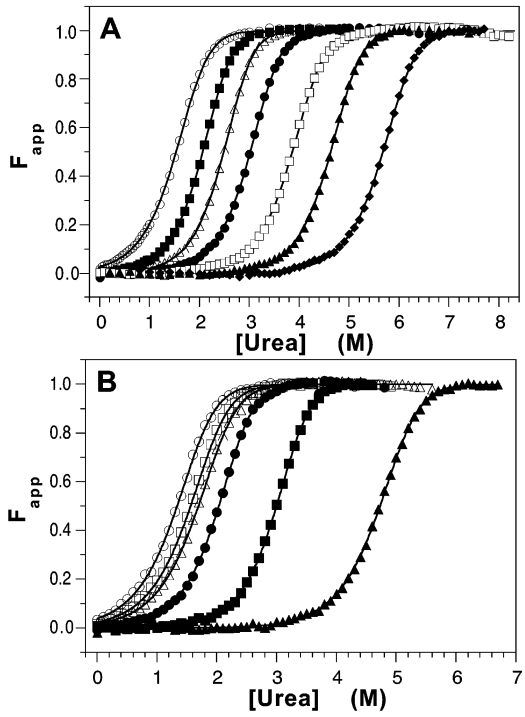

FIGURE 4: Representative urea denaturation transitions for the H2A−H2B dimer at different salt concentrations. (A) Transitions as a function of [KCl]. F_{app} curves are shown for KCl concentrations of 0.1 (○), 0.3 (■), 0.5 (Δ), 0.72 (●), 1.0 (□), 1.5 (▲), and 2.0 M (◆). (B) Transitions as a function of [KI] (open symbols) and [KPi] (solid symbols). F_{app} curves are shown for 0.1 (circles), 0.3 (squares), and 0.6 M (triangles) potassium salt. Conditions: dimer concentration was 10 μM for KCl and KPi, and 5 μM for KI. Buffered with 20 mM potassium phosphate, 0.1 mM EDTA, pH 7.2, 25 °C.

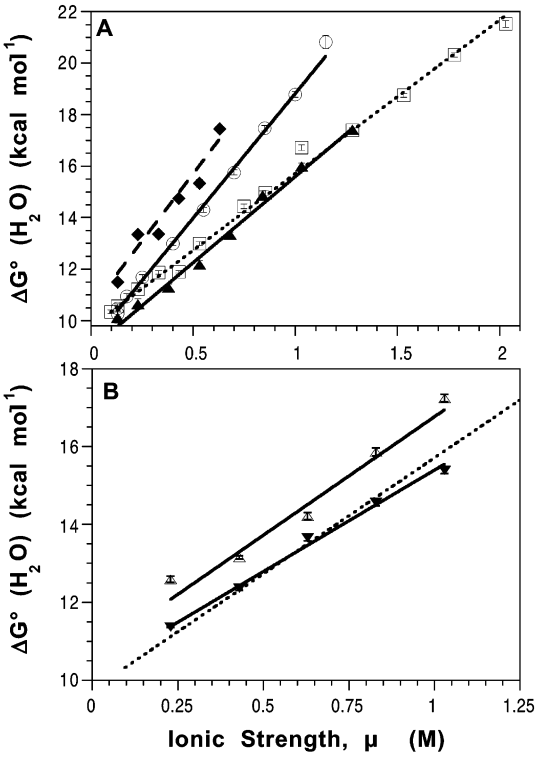

FIGURE 5: The salt dependence of the free energy of unfolding, $\Delta G°(H_2O)$, of the H2A−H2B dimer. The lines represent a linear fit of the data plotted as a function of ionic strength. (A) Subset of potassium salts: K_2SO_4 (◆, dashed line), KPi (○), KOAc (▲), and KCl (□, dotted line). (B) Chloride salts: NaCl (Δ), NH_4Cl (▼), and KCl (dotted line, data shown in panel A). An error of one standard deviation on the error surface for the global fits is shown or is less than the size of the data points. Conditions are given in the legend of Figure 4.

least, as $Na^+ \geq K^+ > NH_4^+$. The small differences in the values of $\Delta(\Delta G°)/\Delta C_\mu$ follow the same relative ranking.

The stabilization of H2A−H2B by KI is in contrast to the typical effect of this salt on proteins. Iodide salts are usually considered protein denaturants (*22*); however, it is clear that KI does have a small, but significant, stabilizing effect on the H2A−H2B dimer (Figures 4 and 6). For the two salts lowest in the Hofmeister series, KBr and KI, the slopes of $\Delta G°(H_2O)$ (Figure 6) and C_M (data not shown) are also linear with the square root of the anion concentration; this linearity is indicative of an electrostatic component to their mode of stabilization (see Discussion).

The effects of salts on several physical parameters of aqueous solutions follow the rank order of the Hofmeister series. Examples include the ability to salt out various hydrophobic molecules or dissolved gases and increasing the surface tension of water (*22*). Figure 7 shows a comparison between the efficacy of the salts in stabilizing H2A−H2B, as measured by $\Delta(\Delta G°)/\Delta C_\mu$, and the ability of the salts to (A) salt out aniline (data compiled in ref *32*) and (B) increase water surface tension (data complied in ref *33*). Literature data is not available for the effect of KPi on these properties of water, and therefore this salt is not included in Figure 7. For both measures of the Hofmeister effect, there is a linear correlation with their stabilization of H2A−H2B.

DISCUSSION

H2A−H2B as a Protein Folding Model System. The data presented in this report demonstrate that the H2A−H2B heterodimer is a suitable model system to address the folding properties of the dimeric histone fold motif. The urea-induced equilibrium unfolding of H2A−H2B is well-described by a two-state mechanism with high reversibility (Figure 3). The two state unfolding of the heterodimer demonstrates that the structure within a given monomer is less stable than the stability provided by the dimeric interface. In other words, the urea concentration necessary to dissociate the two polypeptide chains is also sufficient to unfold the individual chains, preventing the population of partially folded monomers. A similar two-state equilibrium response was observed for the thermal denaturation of the H2A−H2B dimer (*17*).

In the crystal structure of the core nucleosome (*26*), the histone oligomers contain helical structures and sequences that adopt extended conformations that are poorly resolved. Of the 129 residues of the H2A monomer, ∼15 and 31 residues are in the extended N- and C-terminal tails, respectively. Of the 122 residues of the H2B monomer, ∼32 residues are in the N-terminal tail. The well-structured regions of the H2A−H2B heterodimer contain ∼173 residues.

Comparable two-state folding homodimeric systems that have been well-characterized by urea denaturation include the *Arc* repressor of phage P22 (53 residues per monomer) and *E. coli Trp* repressor (106 residues per monomer). Both of these model systems, like the histone fold motif, have dimer interfaces that are intertwined and highly helical (though the *Arc* repressor interface also contains two β-strands). The free energy of urea-induced equilibrium

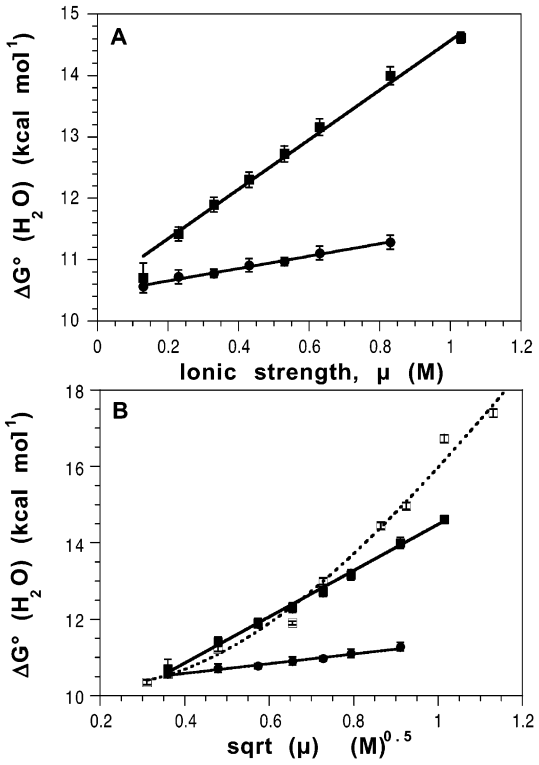

FIGURE 6: The dependence of the free energy of unfolding, $\Delta G°(H_2O)$, of the H2A−H2B dimer on ionic strength for KBr (■) and KI (●). (A) $\Delta G°(H_2O)$ plotted as a function of ionic strength. (B) $\Delta G°(H_2O)$ plotted as a function of the square root of the ionic strength. KCl data (□, dotted line) from Figure 4A is shown for comparison. The lines represent a linear fit of the data; the dotted line for the KCl data is simply drawn to guide the eye and does not indicate a fit of the data. An error of one standard deviation on the error surface for the global fits is shown or is less than the size of the data points. Conditions are given in the legend of Figure 4.

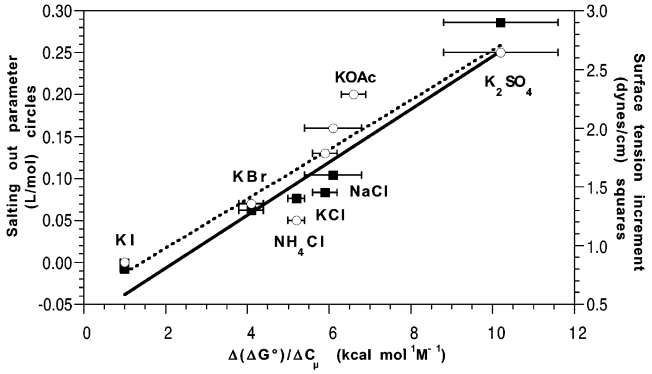

FIGURE 7: Comparison of the ability of various salts to stabilize the H2A−H2B dimer and their effects on two physical properties of aqueous solutions. The surface tension increments for water (■, solid line, right axis) and the ability to salt out aniline (○, dotted line, left axis) are plotted as a function of the increase in free energy of unfolding as a function of ionic strength, $\Delta(\Delta G°)/\Delta C_\mu$ given in Table 1. The lines represent linear fits of the data.

unfolding for the *Arc* repressor is 11 kcal mol^{-1} (25 °C, $\mu \approx 0.3$ M) (*34*). Full-length *Trp* repressor is much more stable, with a $\Delta G°(H_2O)$ value of 22.2 kcal mol^{-1} (25 °C, 0.25 M KCl) (*35*). The isolated dimerization domain of *Trp* repressor, comprising 65 residues per monomer, exhibits a $\Delta G°(H_2O)$ value of 13 kcal mol^{-1} (25 °C in the absence of KCl) (*36*). The $\Delta G°(H_2O)$ value of the H2A−H2B heterodimer, 11.8 kcal mol^{-1}, is comparable to the stability exhibited by the *Arc* repressor and the *Trp* repressor dimerization domain, which have similar interface compositions but somewhat smaller size. An earlier review demonstrated a correlation between the size and conformational stability of dimeric proteins, taking into consideration the structure of the interface (*37*). Addition of data from more recently described protein folding systems supports this observed correlation (Gloss, L. M. (2002) unpublished observations). The H2A−H2B dimer seems to be less stable than one would predict for a protein of its size. Given the basic nature of the histones, it is possible that electrostatic repulsion, particularly from the highly basic N-terminal tails, may destabilize the heterodimer.

Across many protein folding systems, there is a convincing correlation between the *m* value determined from chemical denaturation experiments and the change in solvent-accessible area between the native and unfolded species of proteins, ΔASA (*38*). These authors also demonstrate there is a very strong correlation ($R = 0.994$) between the number of residues in a protein and the ΔASA, which the authors calculated by standard methods from the three-dimensional structures of the proteins and models for unfolded proteins. The only high-resolution structures available for the H2A−H2B dimer are in the presence of the H3−H4 tetramer with or without DNA (*3*, *8*). It is unknown how the structures of the poorly resolved regions of the H2A−H2B dimer, the highly charged N- and C-terminal tails, change in the absence of these highly charged components of the crystal structure. Therefore, we have estimated the ΔASA expected for the unfolding of the isolated heterodimer based on the number of residues in the complex.

If the tails are in an extended, unstructured conformation in both the folded and unfolded species, the ΔASA would arise from the 173 residues in the structured regions. This predicts a ΔASA of 15,800 Å^2 and an *m* value of 2.1 kcal mol^{-1} M^{-1} for urea denaturation. For a protein of 251 residues (including both the well-structured helical regions and the tails of the H2A−H2B dimer), one would expect a ΔASA value of 22,400 Å^2 and an *m* value of 2.8 kcal mol^{-1} M^{-1}. This calculated *m* value is quite consistent with that measured for H2A−H2B unfolding (2.8−2.9 kcal mol^{-1} M^{-1}). This agreement suggests that the poorly structured tails of the H2A−H2B dimer may collapse into a solvent-excluding structure when not complexed with DNA. Such a collapse may stabilize the protein through van der Waal interactions in the collapsed structure as well as releasing water from the hydrophobic moieties of the side-chains in the tails, particularly the aliphatic portions of the Lys and Arg side chains. However, such a collapsed structure would bring the basic residues of the tails into closer juxtaposition than would an extended structure. This hypothesis prompted an investigation of the role of electrostatics in the stability of the H2A−H2B dimer by determining the effects of salts on the stability of the heterodimer to urea denaturation. Furthermore, Ausio and colleagues have shown that acetylation of lysines in the histone H4 tail, with concomitant reduction of positive charge, promoted the formation of helical structure, both in the full-length protein and in peptides corresponding to the N-terminal tail of H4 (*39*). Increasing concentrations of KCl, KPi and the helix-stabilizing cosolvent, trifluroethanol, increase the helical structure in the H2A−H2B dimer (CD spectral data not shown). These cosolute effects are somewhat attenuated in

a tail-less construct of H2A−H2B (described in the following report, Placek and Gloss), suggesting that some of the induced helical structure may arise from the N-terminal tails.

Salt Stabilization of the H2A−H2B Heterodimer. Even if the tails of the isolated H2A−H2B dimer do not adopt a collapsed structure, the role of electrostatic interactions in the stability of the heterodimer is an interesting question. It is unclear if a highly charged, extended/unfolded tail tethered to the structured region of a protein can exert an effect on the stability of the structured region. To address the importance of electrostatics on H2A−H2B stability, the effect of ionic strength on the protein's stability was examined. However, salts can stabilize proteins by effects other than screening of electrostatic repulsion. It is essential to distinguish the different components of salt-induced protein stabilization.

The hydrophobic effect, related to the entropy of the aqueous solvent, is a fundamental driving force in protein folding. Cosolutes, including salts, can make important contributions to the hydrophobic effect and the ability of water to solvate hydrophobic moieties. Timasheff and colleagues demonstrated that salts which stabilize proteins promote preferential hydration, with the exclusion of the salt from the protein surface (reviewed in refs *20* and *21*)). These salts "salt-out" hydrophobic moieties with relative efficacies that follow the Hofmeister series (*40*). Conversely, I^- and guanidinium destabilize proteins, by their ability to "salt-in" the peptide group by interaction with the protein and preferential binding to the unfolded protein, rather than the native state.

Several studies have compared the free energy of folding of proteins at 0 M salt and a single high concentration of salt. However, it is important to assess the effect on stability over a range of salt concentrations. The different mechanisms of salt stabilization can be distinguished by the salt concentration dependence of the thermodynamic parameters describing the protein stability. Electrostatic interactions follow the Debye−Hückel approximation, which predicts that the free energy should vary linearly with the square root of the ionic strength (*23*). Stabilization by solvent effects (preferential hydration or the Hofmeister effect) should exhibit a nearly linear response of free energy with ion concentration (*22*, *23*). Binding of ions to a specific site that can be saturated should exhibit a hyperbolic relationship between stability and ligand concentration. Examples of such salt dependence studies include RNase T1 (*41*, *42*), GCN4 and other leucine zipper peptides (*24*, *43*) and cold shock proteins (*25*).

Thermal denaturation, using CD and differential scanning calorimetry, has been reported previously for the H2A−H2B heterodimer as well as the H3−H4 dimer, populated at pH 4.5 (*17*−*19*). Using NaCl, these authors found a nonlinear response for T_M, the midpoint of thermal unfolding, with respect to ionic strength (*17*, *19*). However, thermal denaturation was less reversible at higher salt concentrations for both histone heterodimeric systems because of protein aggregation at higher salt concentations (*19*). It was unclear to what extent decreased reversibility contributed to the nonlinear increase in T_M. The reversibility of the urea denaturation studies was unaffected by higher salt concentrations, always ≥95% for all of the data reported herein. This higher reversibility permitted more accurate thermodynamic analyses of the effects of salt on the stability of the heterodimer.

Scheme 1

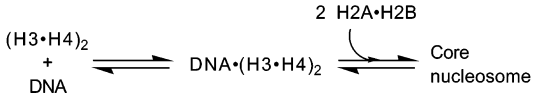

The data presented in this report clearly demonstrate that the salt-induced stabilization of the H2A−H2B dimer arises, in part, from solvent effects by preferential hydration and the Hofmeister effect. The linear dependence of $\Delta G°(H_2O)$ (Figures 5 and 6) and C_M (data not shown) on the ionic strength and salt concentration is support for stabilization by a mechanism via solvent effects. The $\Delta(\Delta G°)/\Delta C_\mu$ values correlate with measures of the Hofmeister effect (Figure 7), such as the ability to salt out aniline or effects on water surface tension.

However, the data also suggest that the stabilization of the H2A−H2B dimer by salts also arises from screening of electrostatic repulsion. The strong and moderate stabilization by KBr and KI is in contrast to the general effects of these salts on other proteins. This is particularly true for KI, which is generally considered as a mild protein denaturant, but stabilizes the H2A−H2B dimer. In addition, these salts exhibit a stabilization that is linear with the square root of the ionic strength, as predicted by the Debye−Hückel approximation (Figure 6). Non-Hofmeister effects of salts on histone proteins have been shown previously, for example on isolated H4 (*44*). It is tempting to ascribe stabilization by screening of electrostatic repulsion to the highly charged N-terminal tails.

Conclusions and Implications for the Biological Function of the Histone Dimer in the Nucleosome. The data presented in this report support the following conclusions:

(1) Like the thermal denaturation of H2A−H2B, the urea-induced unfolding of the dimer is well-described by a two-state mechanism. This is in contrast to other intertwined helical dimers, such as the *Arc* repressor *(45*, *46)* and *Trp* repressor (*36*), which can unfold by two and three state mechanisms when different denaturation methods are employed.

(2) The *m* values suggest that the N-terminal tails of H2A and H2B adopt collapsed, solvent-excluding conformations in the absence of DNA.

(3) Preferential hydration/the Hofmeister effect are important in the salt-induced stabilization of the H2A−H2B dimer. However, there is strong evidence that electrostatic repulsion plays a role in destabilizing the dimer. These data suggest that the stability of the well-structured, helical regions of a protein can be altered by the close juxtaposition of a highly charged, poorly structured region. This conclusion is supported in the following report (Placek and Gloss).

Data from studies of isolated nucleosomes and reconstituted eukaryotic replication systems have demonstrated that the nucleosome is assembled in a stepwise manner (*47*−*49*). Initially, an H3−H4 tetramer binds to DNA, and then subsequently two H2A−H2B dimers bind to the complex: In this assembly, issues of protein folding and stability are intimately related to biological function. If the uncomplexed histone oligomers are stabilized, the equilibria shown in Scheme 1 will be shifted to the left—away from the

thermodynamically favored state of the fully assembled nucleosome. Such stabilization may have a small thermodynamic difference, but more pronounced effects on the kinetics of the dynamics of the nucleosome. The overall effect would be to enhance the transient accessibility of DNA from the surface of the nucleosome, such as proposed by Widom and colleagues in the "site-exposure" model (*50*, *51*), accentuating the transient population of species to the left in Scheme 1. Removal or acetylation of the histone tails does have a small but significant effect on the accessibility of nucleosomal DNA (*52*, *53*). It is known that transcriptionally active chromatin is often hyperacetylated and contains nucleosomes depleted in H2A and H2B (*54*, *55*). A recent report suggests that RNA Pol II can displace H2A−H2B dimers (*56*).

Lysine acetylation results in the removal of positive charge from the highly basic N-terminal tails of the histones. The data in this report suggests that electrostatic repulsion destabilizes the H2A−H2B dimer. It is speculated that this destabilization arises, at least in part, from the high charge density of the N-terminal tails, the sites of acetylation in vivo. To test this hypothesis, we have studied the stability of H2A−H2B variants with one or both N-terminal tails removed (following paper, Placek and Gloss).

ACKNOWLEDGMENT

We dedicate this paper to the memory of our late colleague, Jeremy N.S. Evans, in appreciation for his friendship and scientific insights and guidance. The pET overexpression vectors were kindly provided by Drs. Karolin Luger (now at Colorado State University) and Timothy Richmond of the Instititute for Molecular Biology and Biophysics at the ETHZ, Zurich, Switzerland. The assistance of Ms. Gail E. Deckert in the purification of the recombinant histones used in this study is gratefully acknowledged. We appreciate helpful discussions and critical reading of the manuscript by Traci Topping and Dr. Michael J. Smerdon.

REFERENCES

1. Workman, J. L., and Kingston, R. E. (1998) Alteration of nucleosome structure as a mechanism of transcriptional regulation, *Annu. Rev. Biochem. 67*, 545−79.
2. Wolffe, A. P., and Guschin, D. (2000) Chromatin structural features and targets that regulate transcription, *J. Struct. Biol. 129*, 102−122.
3. Arents, G., Burlingame, R. W., Wang, B. C., Love, W. E., and Moudrianakis, E. N. (1991) The nucleosomal core histone octamer at 3.1 Å resolution: a tripartite protein assembly and a left-handed superhelix, *Proc. Natl. Acad. Sci. U.S.A. 88*, 10148−52.
4. Arents, G., and Moudrianakis, E. N. (1995) The histone fold: A ubiquitous architectural motif utilized in DNA compaction and protein dimerization, *Proc. Natl. Acad. Sci. U.S.A. 92*, 11170−74.
5. Baxevanis, A. D., Arents, G., Moudrianakis, E. N., and Landsman, D. (1995) A variety of DNA-binding and multimeric proteins contain the histone fold motif, *Nucleic Acids Res. 23*, 2685−2691.
6. Xie, X., Kokubo, T., Cohen, S. L., Mirza, U., Hoffmann, A., Chait, B. T., Roeder, R. G., Nakatani, Y., and Burley, S. K. (1996) Structural similarity between TAFs and the heterotetrameric core of the histone octamer, *Nature 380*, 316−322.
7. Birck, C., Poch, O., Romier, C., Ruff, M., Mengus, G., Lavigne, A. C., Davidson, I., and Moras, D. (1998) Human $TAF_{II}28$ and $TAF_{II}18$ interact through a histone fold encoded by atypical evolutionary conserved motifs also found in the SPT3 family, *Cell 94*, 239−49.
8. Luger, K., Mader, A. W., Richmond, R. K., Sargent, D. F., and Richmond, T. J. (1997) Crystal structure of the nucleosome core particle at 2.8 A resolution, *Nature 389*, 251−60.
9. Cheung, P., Allis, C. D., and Sassone-Corsi, P. (2000) Signaling to chromatin through histone modifications, *Cell 103*, 263−71.
10. Strahl, B. D., and Allis, C. D. (2000) The language of covalent histone modifications, *Nature 403*, 41−5.
11. D'Anna, J. A., and Isenberg, I. (1974) A histone cross-complexing pattern, *Biochemistry 13*, 4992−4997.
12. Isenberg, I. (1979) Histones, *Annu. Rev. Biochem. 48*, 159−91.
13. van Holde, K. (1989) *Chromatin*, Springer-Verlag, New York.
14. Eickbush, T. H., and Moudrianakis, E. N. (1978) The histone core complex: An octamer assembled by two sets of protein−protein interactions, *Biochemistry 17*, 4955−64.
15. Benedict, R. C., Moudrianakis, E. N., and Ackers, G. K. (1984) Interactions of the nucleosomal core histones: A calorimetric study of octamer assembly, *Biochemistry 23*, 1214−18.
16. Godfrey, J. E., Baxevanis, A. D., and Moudrianakis, E. N. (1990) Spectropolarimetric analysis of the core histone octamer and its subunits, *Biochemistry 29*, 965−972.
17. Karantza, V., Baxevanis, A. D., Freire, E., and Moudrianakis, E. N. (1995) Thermodynamic studies of the core histones: Ionic strength and pH dependence of H2A−H2B dimer stability, *Biochemistry 34*, 5988−96.
18. Karantza, V., Freire, E., and Moudrianakis, E. N. (1996) Thermodynamic studies of the core histones: pH and ionic strength effects on the stability of the $(H3-H4)/(H3-H4)_2$ system, *Biochemistry 35*, 2037−46.
19. Karantza, V., Freire, E., and Moudrianakis, E. N. (2001) Thermodynamic studies of the core histones: Stability of the octamer subunits is not altered by removal of their terminal domains, *Biochemistry 40*, 13114−123.
20. Timasheff, S. N. (1993) The control of protein stability and association by weak interactions with water: How do solvents affect these processes? *Annu. Rev. Biophys. Biomol. Struct. 22*, 67−97.
21. Timasheff, S. N. (1998) Control of protein stability and reactions by weakly interacting cosolvents: The simplicity of the complicated, *Adv. Protein Chem. 51*.
22. Baldwin, R. L. (1996) How Hofmeister ion interactions affect protein stability, *Biophys. J. 71*, 2056−63.
23. Record, M. T., Jr., Zhang, W., and Anderson, C. F. (1998) Analysis of effects of salts and uncharged solutes on protein and nucleic acid equilibria and processes: A practical guide to recognizing and interpreting polyelectrolyte effects, Hofmeister effects and osmotic effects of salts, *Adv. Protein Chem. 51*, 282−355.
24. Kenar, K. T., Garcia-Moreno, B., and Freire, E. (1995) A calorimetric characterization of the salt dependence of the stability of the GCN4 leucine zipper, *Protein Sci. 4*, 1934−38.
25. Perl, D., and Schmid, F. X. (2001) Electrostatic stabilization of a thermophilic cold shock protein, *J. Mol. Biol. 313*, 343−357.
26. Luger, K., Rechsteiner, T. J., Flaus, A. J., Waye, M. M., and Richmond, T. J. (1997) Characterization of nucleosome core particles containing histone proteins made in bacteria, *J. Mol. Biol. 272*, 301−311.
27. Mann, C. J., and Matthews, C. R. (1993) Structure and stability of an early folding intermediate of *Escherichia coli* trp aporepressor measured by far-UV stopped-flow circular dichroism and 8-anilino-1-naphthalene sulfonate binding, *Biochemistry 32*, 5282−5290.
28. Pace, C. N. (1986) Determination and analysis of urea and guanidine hydrochloride denaturation curves, *Methods Enzymol. 131*, 266−280.
29. Zitzewitz, J. A., Bilsel, O., Luo, J., Jones, B. E., and Matthews, C. R. (1995) Probing the folding mechanism of a leucine zipper peptide by stopped-flow circular dichroism spectroscopy, *Biochemistry 34*, 12812−12819.
30. Bilsel, O., Zitzewitz, J. A., Bowers, K. E., and Matthews, C. R. (1999) Folding mechanism of the alpha-subunit of tryptophan synthase, an alpha/beta barrel protein: global analysis highlights the interconversion of multiple native, intermediate, and unfolded forms through parallel channels, *Biochemistry 38*, 1018−29.
31. Beechem, J. M. (1992) Global analysis of biochemical and biophysical data, *Methods Enzymol. 210*, 37−54.
32. Long, F. A., and McDevit, W. F. (1952) Activity coefficients of nonelectrolyte solutes in aqueous salt solutions, *Chem. Rev. 51*, 119−169.

33. Ebel, C., Faou, P., Kernel, B., and Zaccai, G. (1999) Relative role of anions and cations in the stabilization of halophilic malate dehydrogenase, *Biochemistry 38*, 9039−9047.
34. Milla, M. E., and Sauer, R. T. (1995) Critical side-chain interactions at a subunit interface in the arc repressor dimer, *Biochemistry 34*, 3344−3351.
35. Gloss, L. M., Simler, B. R., and Matthews, C. R. (2001) Rough energy landscapes in protein folding: Dimeric E. coli Trp repressor folds through three parallel channels, *J. Mol. Biol. 312*, 1121−1134.
36. Gloss, L. M., and Matthews, C. R. (1997) Urea and thermal equilibrium denaturation studies on the dimerization domain of *Escherichia coli Trp* repressor, *Biochemistry 36*, 5612−5623.
37. Neet, K. E., and Timm, D. E. (1994) Conformational stability of dimeric proteins: Quantitative studies by equilibrium denaturation, *Protein Sci. 3*, 2167−2174.
38. Myers, J. K., Pace, C. N., and Scholtz, J. M. (1995) Denaturant *m* values and heat capacity changes: Relation to changes in accessible surface areas of protein folding, *Protein Sci. 4*, 2138−2148.
39. Wang, X., Moore, S. C., Laszckzak, M., and Ausió, J. (2000) Acetylation increases the α-helical content of the histone tails of the nucleosome, *J. Biol. Chem. 275*, 35013−35020.
40. Hofmeister, F. (1888) Zur Lehre von der Wirkung der Salze. II, *Arch. Exp. Pathol. Pharmakol. 24*, 247−260.
41. Pace, C. N., and Grimsley, G. R. (1988) Ribonuclease T1 is stabilized by cation and anion binding, *Biochemistry 27*, 3242−46.
42. Hu, C.-Q., Sturtevant, J. M., Thomson, J. A., Erickson, R. E., and Pace, C. N. (1992) Thermodynamics of ribonuclease T1 denaturation, *Biochemistry 31*, 4876−4882.
43. Kohn, W. D., Kay, C. M., and Hodges, R. D. (1997) Salt effects on protein stability: Two-stranded α-helical coiled-coils containing inter- or intrahelical ion pairs, *J. Mol. Biol. 267*, 1039−1052.
44. Wickett, R. R., Li, H. J., and Isenberg, I. (1972) Salt effects on Histone IV conformation, *Biochemistry 11*, 2952−2957.
45. Robinson, C. R., Rentzeperis, D., Silva, J. L., and Sauer, R. T. (1997) Formation of a denatured dimer limits the thermal stability of *Arc* repressor, *J. Mol. Biol, 273*.
46. Silva, J. L., Silveira, C. F., Correia, A., and DuPontes, L. (1992) Dissociation of a native dimer to a molten globule monoomer. Effects of pressure and dilution on the association equilibrium of *Arc* repressor, *J. Mol. Biol. 223*, 545−555.
47. Oohara, I., and Wada, A. (1987) Spectroscopic studies on histone-DNA interactions. II. Three transitions in nucleosomes resolved by salt-titration, *J. Mol. Biol. 196*, 399−411.
48. Smith, S., and Stillman, B. (1991) Stepwise assembly of chromatin during DNA replication *in vitro*, *EMBO J. 10*, 971−980.
49. Ishimi, Y., Sugasawa, K., Hanaoka, F., and Kikuchi, A. (1991) Replication of the Simian Virus 40 chromosome with purified proteins, *J. Biol. Chem. 266*, 16141−16148.
50. Widom, J. (1998) Structure, dynamics, and function of chromatin in vitro, *Annu. Rev. Biophys. Biomol. Struct. 27*, 285−327.
51. Polach, K. J., and Widom, J. (1999) Restriction enzymes as probes of nucleosome stability and dynamics, *Methods Enzymol. 304*, 278−98.
52. Polach, K. J., Lowary, P. T., and Widom, J. (2000) Effects of core histone tail domains on the equilibrium constants for dynamic DNA site accessibility in nucleosomes, *J. Mol. Biol. 298*, 211−23.
53. Anderson, J. D., Lowary, P. T., and Widom, J. (2001) Effects of histone acetylation on the equilibrium accessibility of nucleosomal DNA target sites, *J. Mol. Biol. 307*, 977−85.
54. Hansen, J. C., and Wolffe, A. P. (1994) A role for histones H2A/H2B in chromatin folding and transcriptional repression, *Proc. Natl. Acad. Sci. U.S.A. 91*, 2339−2343.
55. Wolffe, A. P. (1994) Transcription: in tune with the histones, *Cell 77*, 13−16.
56. Kireeva, M. L., Walter, W., Tchernajenko, V., Bondarenko, V., Kashlev, M., and Studitsky, V. M. (2002) Nucleosome Remodeling Induced by RNA Polymerase II. Loss of the H2A/H2B Dimer during Transcription, *Mol. Cell 9*, 541−52.
57. Kraulis, P. J. (1991) MOLSCRIPT: a program to produce both detailed and schematic plots of protein structures, *J. Appl. Crystallogr. 24*, 946−950.

BI026282S